buildings

MDPI

Article

Modal Identification of a Superimposed Structure: The Crossing of the Mosque–Cathedral of Córdoba

Natalia Fernández-Pérez [1,*], María Victoria Requena-García-Cruz [1,2], Isabel González-de-León [2,3] and Antonio Morales-Esteban [1,2]

[1] Department of Building Structures and Geotechnical Engineering, University of Seville, Av. Reina Mercedes 2, 41012 Seville, Spain; mrequena1@us.es (M.V.R.-G.-C.); ame@us.es (A.M.-E.)
[2] Instituto Universitario de Arquitectura y Ciencias de la Construcción (IUACC), University of Seville, Av. Reina Mercedes 2, 41012 Seville, Spain; isabel.gonzalezdeleon@gm.uca.es
[3] Department of Mechanical Engineering and Industrial Design, University of Cadiz, Campus Universitario de Puerto Real, Av. Universidad de Cádiz 10, 11519 Puerto Real, Spain
* Correspondence: nfernandez2@us.es

Abstract

The Gothic–Renaissance crossing of the Mosque–Cathedral of Córdoba constitutes one of the most structurally complex sectors of the monument owing to the coexistence of Islamic and Christian construction systems developed over several centuries. Accurately reproducing the mechanical interaction between these successive construction phases remains a major challenge in the numerical assessment of historically superimposed heritage structures. This study presents the first three-dimensional finite element (FE) model of the crossing, explicitly representing the interfaces between the Gothic–Renaissance intervention and the surrounding Islamic structure through frictional contact elements implemented in OpenSees 3.7.2. The model incorporates the principal structural components of the crossing, including the masonry walls and piers, ribbed vaults, dome, buttresses and adjacent Islamic arcades. Mesh and material sensitivity analyses were performed to quantify the influence of the principal modelling parameters on the predicted dynamic response and to establish an efficient and reliable numerical model. The results showed that the first three natural frequencies vary by less than 0.7% with mesh refinement, whereas ±10% variations in density or Young's modulus modify the predicted frequencies by approximately 5% without altering the modal hierarchy. The first three vibration modes correspond to two dominant translational modes (2.01 Hz and 2.52 Hz) followed by a torsional mode (3.14 Hz), demonstrating that the crossing and the surrounding Islamic structure behave as a single integrated structural system rather than as independent construction phases. Higher vibration modes reveal localized deformation mechanisms concentrated in the buttresses, whose modal behavior is consistent with the historical strengthening interventions that modified their stiffness.

Keywords: Mosque–Cathedral of Córdoba; Gothic–Renaissance crossing; finite element modelling; historical interfaces; modal analysis; heritage structures

Check for updates

Academic Editor: Salvatore Verre

Received: 31 July 2026
Revised: 25 September 2026
Accepted: 1 October 2026
Published: 6 October 2026

Copyright: © 2026 by the authors. Licensee MDPI, Basel, Switzerland. This article is an open access article distributed under the terms and conditions of the Creative Commons Attribution (CC BY) license.

1. Introduction

1.1. Challenges in Modelling Complex Heritage Buildings

The structural assessment of architectural heritage increasingly relies on finite element (FE) modelling to investigate the mechanical behavior of historical structures and to support their conservation, rehabilitation, and seismic assessment strategies [1]. Advances in

computational resources and numerical methods have enabled the development of gradually sophisticated FE models capable of representing complex geometries, heterogeneous materials, and nonlinear structural behavior [2,3]. Nevertheless, developing representative numerical models for heritage buildings remains a major challenge due to uncertainties associated with geometry, construction techniques, material properties, and long-term structural evolution [1,2].

Although finite element modelling (FEM) is widely used for modelling geometrically complex heritage structures, other numerical strategies can provide robust solutions for specific structural problems. Wang et al. [4] proposed a generalized finite difference method for the stress analysis, while Kabir and Aghdam [5] developed a Bézier-based multi-step method for nonlinear vibration problems. Although demonstrated for composite materials and beams rather than historical masonry monuments, these methods illustrate the broader range of numerical approaches available for structural analysis.

Unlike modern buildings, heritage structures are rarely the result of a single construction phase. Instead, they usually evolve over centuries through successive enlargements, repairs, partial demolitions, changes in use, and strengthening interventions. Consequently, their current structural behavior depends not only on the properties of the constituent materials but also on the interaction between structural systems belonging to different historical periods [6]. These transformations frequently introduce discontinuities in stiffness, mass distribution, geometry, and load-transfer mechanisms that are difficult to represent numerically, particularly in complex monuments with different structural typologies coexisting within the same construction [7].

The mechanical characterization of historical masonry introduces an additional level of complexity. Material properties are commonly affected by construction techniques, weathering, and deterioration. However, in this type of buildings, destructive testing is generally restricted [1,8]. Therefore, the mechanical parameters adopted in FE models are typically derived from previous experimental investigations, non-destructive testing campaigns, technical standards, or literature values, introducing unavoidable uncertainty into the numerical representation of the structure [9].

Recent studies have demonstrated that modelling assumptions can significantly influence the predicted structural response. Variations in material properties, boundary conditions, and mesh discretization may produce noticeable changes in the dynamic characteristics of masonry structures, highlighting the importance of sensitivity analyses during the development of reliable FE models [10].

The reliability of current FE modelling approaches is reflected in recent applications to medieval churches [11,12], monumental masonry towers [13], cathedral structures such as Milan Cathedral [14] and Notre-Dame de Paris [15,16], and historical masonry vaults subjected to static and seismic loading [17–19]. Further studies have combined detailed 3D FE modelling with modal identification and nonlinear assessment in the Casamari Gothic Church [20], whose scale, vertical development and geometrical complexity are comparable to those of the Gothic–Renaissance crossing. However, most of these studies focus on individual structural systems. Numerical models explicitly accounting for the interaction between construction phases in historically layered monuments remain comparatively scarce.

1.2. Numerical Modelling of Historically Layered Monuments

Monuments composed of multiple construction phases represent one of the most demanding applications of FE modelling because their structural response depends on the interaction between systems built at different periods [21]. While the global behavior of each construction phase may be represented adequately, reproducing the mechanical

interaction across historical interfaces remains a significant challenge. In many numerical models, these interfaces are idealized by assuming perfect continuity between adjacent structural components or are simply neglected [22]. Hence, this can potentially lead to unrealistic stiffness distributions and inaccurate load-transfer mechanisms [21].

For large and geometrically complex monuments, macro-modelling approaches are generally preferred because they provide a suitable compromise between computational efficiency and structural accuracy [11,12]. However, the simplifications inherent to these models make it difficult to reproduce local interaction mechanisms between successive construction phases. This limitation becomes even more critical in vaulted masonry structures, whose 3D load-transfer mechanisms remain difficult to simulate accurately under static and seismic loading [13,16,18,19].

The Mosque–Cathedral of Córdoba is an outstanding example of this type of historically layered monument. The construction of the Gothic–Renaissance crossing during the sixteenth century introduced a massive vertical structure into the pre-existing Islamic hypostyle hall without replacing its original structural system. As a result, the present structural configuration is governed by the interaction between two construction systems characterized by different geometries, materials, structural typologies and load-bearing mechanisms (including masonry vaults, arches and pillars). This makes the crossing one of the most structurally complex sectors of the monument.

Although previous studies by the authors have investigated the structural and seismic behavior of other sectors of the Mosque–Cathedral, particularly the Abd al-Rahman I sector [23–25], no detailed 3D FE model of the Gothic–Renaissance crossing has yet been developed. Moreover, the mechanical interaction between the Christian intervention and the surrounding Islamic fabric has not been investigated explicitly, representing an important gap in the numerical assessment of the monument.

1.3. Dynamic Characterization as a Basis for Structural Assessment

The dynamic behavior of a structure provides valuable information about its global stiffness distribution and structural interaction. Modal properties, such as natural frequencies and vibration modes, are particularly sensitive to variations in geometry, material properties and boundary conditions. Therefore, modal analysis can be used as an effective tool for evaluating the consistency of FE models before nonlinear analyses, seismic assessment or model updating procedures are undertaken [10,14].

Since the predicted dynamic response depends directly on the adopted modelling assumptions, it is essential to evaluate the influence of the principal numerical parameters during model development. Recent studies on complex heritage structures, including Milan Cathedral and Notre-Dame de Paris Cathedral, have demonstrated that the adopted elastic properties, modelling strategies and structural idealizations significantly affect the predicted modal characteristics [15–17]. Likewise, investigations on historical masonry vaults have highlighted the influence of mesh discretization on both computational efficiency and numerical accuracy [26].

Consequently, preliminary sensitivity analyses constitute an essential stage in the development of reliable FE models. By identifying the modelling parameters that most strongly influence the dynamic response, they provide a robust basis for subsequent model updating procedures and advanced structural and seismic assessments.

1.4. Scope of This Study

This paper presents a 3D FE model of the Gothic–Renaissance crossing of the Mosque–Cathedral of Córdoba, one of the most structurally complex sectors of the monument due to the coexistence of Islamic and Christian construction systems. The study addresses

one of the principal challenges in the numerical modelling of historically layered monuments: the realistic representation of the mechanical interaction between successive construction phases.

To overcome this limitation, the proposed model explicitly represents the interfaces between the Gothic–Renaissance crossing and the surrounding Islamic structure using frictional contact elements implemented in OpenSees [27] through the 'ZeroLengthContactASDimplex' formulation [28]. This approach provides a more realistic representation of the load-transfer mechanisms across historical interfaces than the conventional assumption of perfect continuity. Although contact formulations have considerably expanded the capabilities of FE modelling, their application to large-scale heritage monuments remains limited. To the best of the authors' knowledge, this work represents one of the few reported applications of the 'ZeroLengthContactASDimplex' formulation to a heritage monument of this scale and structural complexity.

The objectives of this study are threefold. First, to develop a representative 3D FE model of the Gothic–Renaissance crossing, including the explicit representation of the interaction between its principal structural components. Second, to investigate the influence of mesh discretization and the principal mechanical parameters on the predicted dynamic response through systematic sensitivity analyses. Finally, to establish a reliable numerical framework for the dynamic characterization of the crossing by identifying both global and local vibration mechanisms, evaluating their relationship with the current structural configuration and the historical evolution of the monument, and identifying potential local deformation patterns involving individual structural components.

It should be noted that the authors previously performed a comparison between linear and nonlinear analyses under gravitational loading [29]. The results showed essentially identical displacement distributions in both simulations, indicating that the structure remains within the elastic range. Therefore, the nonlinear formulation does not influence the modal results presented here.

The proposed methodology establishes a robust numerical framework for future model updating, nonlinear structural analyses and a seismic assessment of the Mosque–Cathedral of Córdoba. More broadly, it provides a transferable strategy for the numerical modelling of historically layered heritage monuments in which the interaction between successive construction phases governs the global structural response.

2. Case Study: The Chapter of the Mosque–Cathedral of Córdoba

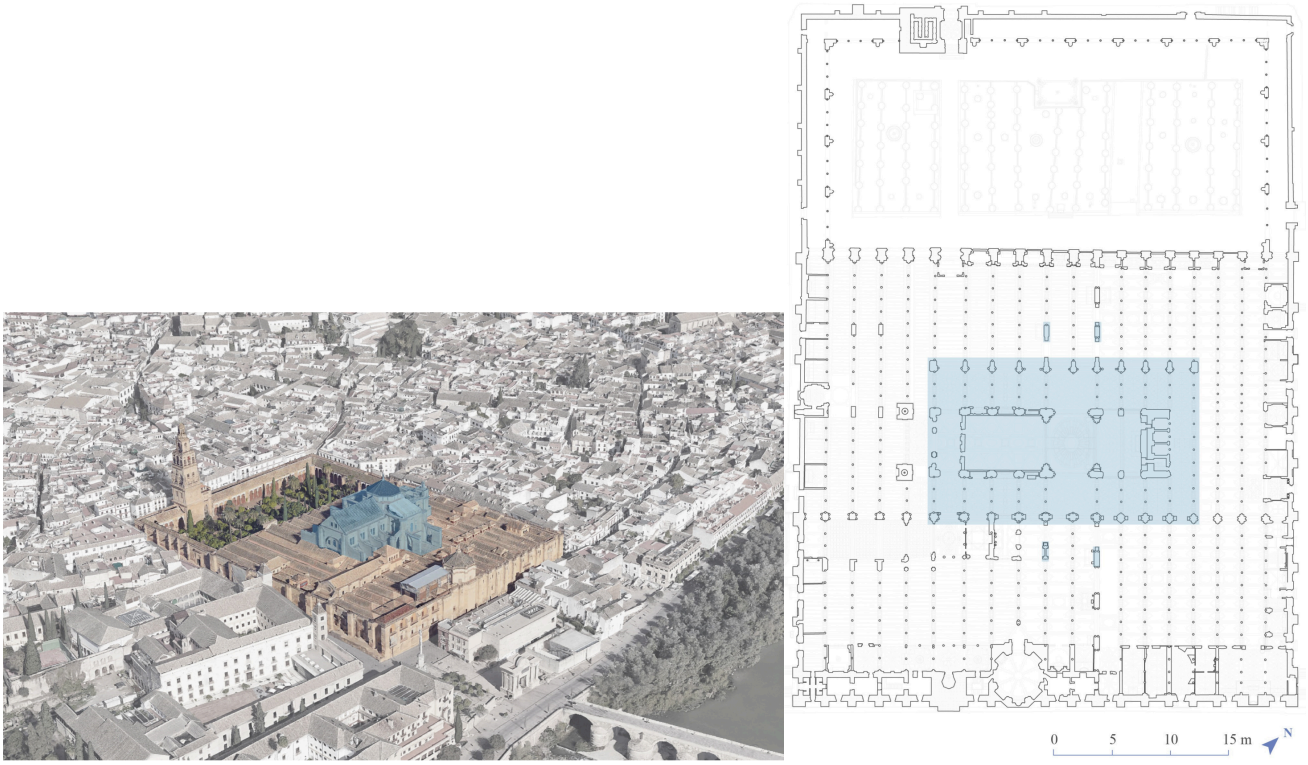
2.1. History Evolution

The Chapter of the Mosque–Cathedral of Córdoba constitutes one of the most significant transformations undergone by the monument throughout its long construction history (Figure 1a). Its current configuration is primarily the result of the insertion of the Gothic–Renaissance crossing, presbytery, and choir within the pre-existing Islamic hypostyle hall during the sixteenth century (Figure 1b). This intervention introduced a new architectural and structural system into a building that had already undergone several major construction phases.

The Islamic Mosque originated in 785 under Abd al-Rahman I and was subsequently enlarged through successive interventions that progressively extended the hypostyle hall while maintaining its predominantly modular organization [30]. Following the Christian conquest of Córdoba in 1236, the building was consecrated as a cathedral and progressively adapted to Christian worship.

The most significant transformation of the former prayer hall began in the sixteenth century with the construction of the crossing complex in its central area. The intervention, initiated under the direction of Hernán Ruiz I and completed in 1607, introduced the Gothic–

Renaissance crossing, presbytery, and choir within the pre-existing Islamic structure. Rather than constituting an independent construction, the new modification was adapted to the modular organization of the mosque and incorporated structural alignments inherited from its successive construction phases.



(**a**) (**b**)

Figure 1. Mosque–Cathedral of Córdoba and location of the study area: (**a**) general view of the monument adapted from Google Earth [31]; and (**b**) plan of the Mosque–Cathedral drawn by the authors based on the work from [32]. In blue, the Gothic–Renaissance crossing is highlighted.



(**a**) (**b**)

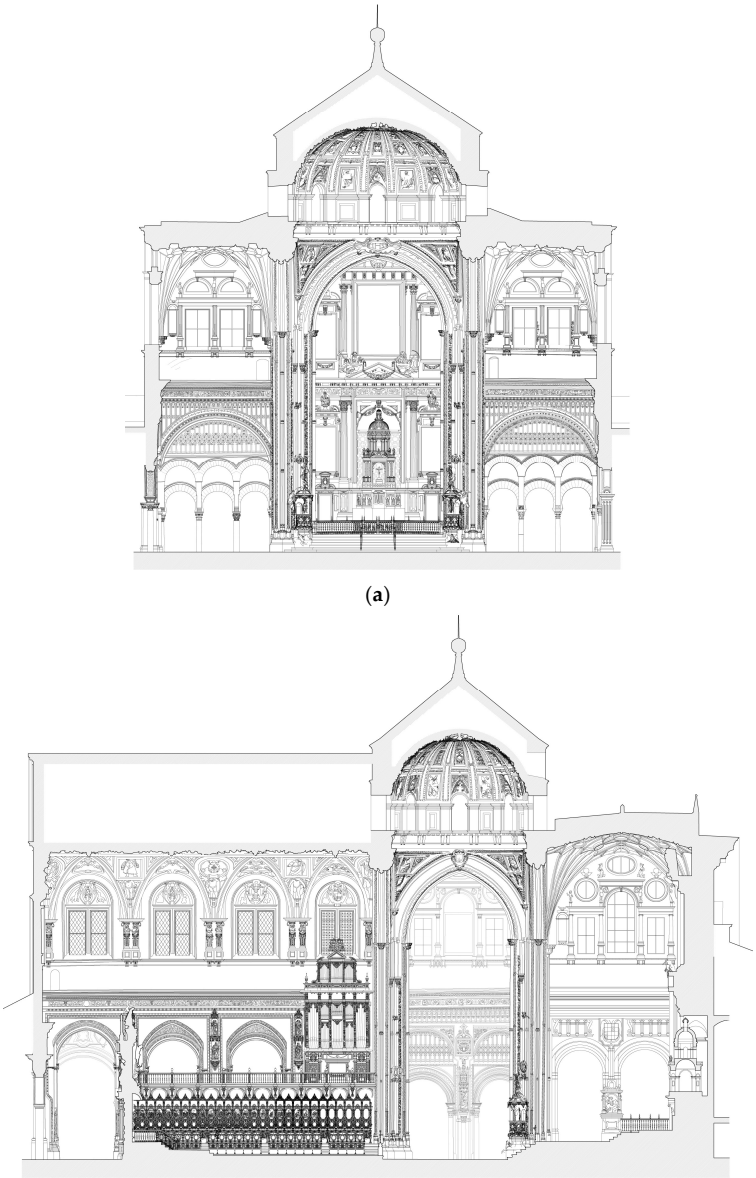
Figure 2. Geometrical configuration and historical superposition of the study area: (**a**) pre-existing Islamic structural system, and (**b**) Gothic–Renaissance intervention and resulting interaction between successive construction phases. Pictures taken by the authors.

The resulting configuration constitutes a particularly complex example of architectural and structural superposition (Figure 2). The predominantly horizontal organization of the Islamic hypostyle hall coexists with the considerably taller and more massive Gothic–Renaissance structure. Hence, a direct interaction is generated between structural elements belonging to different historical periods and conceived according to different construction techniques.

2.2. Geometrical Configuration and Construction Phases

The study area comprises the Gothic–Renaissance crossing and the adjacent sectors of the Islamic Mosque involved in its structural configuration (Figure 2b). The crossing follows a Latin-cross plan formed by the central crossing bay and the longitudinal and transverse arms extending towards the choir, presbytery, and lateral sectors (Figure 1).

Its geometry is characterized by a pronounced vertical development, with the central dome rising above the vaulted systems of the surrounding arms (Figure 3).



(**a**)

(**b**)

Figure 3. Configuration of the Gothic–Renaissance crossing and interaction between construction phases: (**a**) transversal (drawn by the authors based on the work from [33]; and (**b**) longitudinal (drawn by the authors based on the work from [34]).

The lower levels retain structural elements belonging to the previous Islamic construction phases. Columns and superimposed arcades are preserved beneath and around the Gothic–Renaissance structure, resulting in a complex geometrical transition between the massive supports of the crossing and the smaller-scale repetitive elements of the former hypostyle hall. The distribution of these elements is not uniform throughout the study area, as the crossing extends over sectors corresponding to different enlargements of the mosque.

The interaction between the two construction systems is particularly evident at the lower levels of the crossing. The massive supports of the Gothic–Renaissance structure were arranged in relation to the existing columns and arcades to enable the transfer of loads towards the foundations [35].

2.3. Structural System and Construction Characteristics

The crossing consists of massive masonry walls and piers supporting a system of arches, ribbed vaults, and the central dome. Unlike conventional cathedral crossings, the vertical supports of the Gothic–Renaissance intervention are not founded on an entirely new structural scheme. Instead, they were arranged to coincide, whenever possible, with the existing modular layout of the mosque, allowing part of the load path to be transmitted through pre-existing columns, arcades, and masonry elements.

The study area incorporates a wide variety of structural components, including stone columns, masonry piers, horseshoe and semicircular arches, ribbed vaults (Figure 4a), buttresses (Figure 4b), and the central dome (Figure 2b). The coexistence of different materials, construction techniques, and structural typologies results in significant variations in stiffness, mass distribution, and load-transfer mechanisms, making this area one of the most complex sectors of the monument from a structural perspective.



(**a**) (**b**)

Figure 4. Details of constructive features: (**a**) Interior view of the Mosque, and (**b**) external part of the Cathedral. Pictures taken by the authors.

3. Numerical Model

3.1. Geometrical Model

The model of the Gothic–Renaissance crossing has been developed using AutoCad 2026 3D CAD software [36], integrating historical plans and direct site observations. The model reproduces the principal structural components involved in the global behavior of the study area, including the masonry walls and piers, arches, ribbed vaults, central dome, buttresses, and the lower-level Islamic arcades (Figure 5).

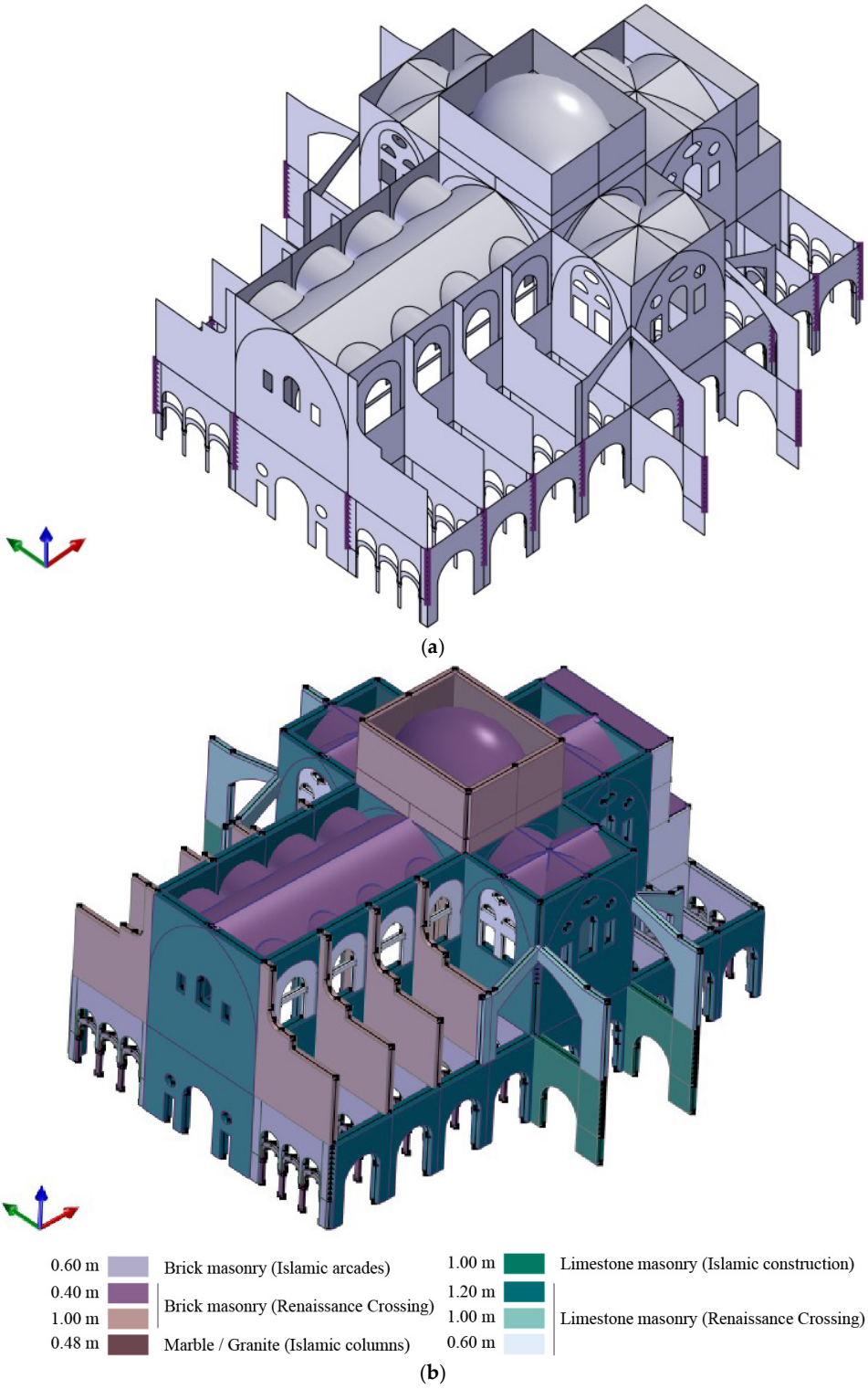


Figure 5. FE model. (**a**) Geometry, and (**b**) constitutive materials and thicknesses.

The geometry and thicknesses of the principal structural components were established through a review and cross-comparison of historical descriptions, architectural plans and detailed sections of the monument. The main documentary sources were the historical study by Hernández Giménez [31], the transverse and longitudinal sections of the Gothic–Renaissance crossing drawn by Almagro Gorbea [33,34] and the 2020 Management Plan of the Mosque–Cathedral of Córdoba [37]. Where accessible, selected visible dimensions were verified through on-site measurements. The thicknesses of inaccessible internal elements were inferred from the cross-comparison of the documentary sources described above.

To ensure a computationally efficient FE model while preserving the global structural behavior, some geometrical simplifications have been introduced. The geometrical idealization follows modelling strategies previously applied by the authors to the Mosque–Cathedral of Córdoba [23] and the Giralda of Seville [13], in which the principal load-bearing components were retained while minor architectural and decorative details were omitted to investigate the global structural response. Non-structural architectural details, ornamental features, moldings, capitals, and decorative elements have been omitted, whereas irregular geometries have been idealized using simplified surfaces and volumes. It has been checked that these simplifications reduce the computational cost without significantly affecting the global stiffness or mass distribution of the structure.

The model represents the interaction between the Gothic–Renaissance crossing and the pre-existing Islamic structure by means of interface elements. The interface elements, represented by the purple lines along the perimeter of the numerical models in Figures 5a and 6, were introduced in the X and Y directions, where applicable, at the contact boundaries between both structures, respecting the existing geometry. Particular attention has been paid to the representation of the lower-level arcades, where the later masonry supports interact with the original structural system and significantly influence the transfer of vertical and horizontal loads.

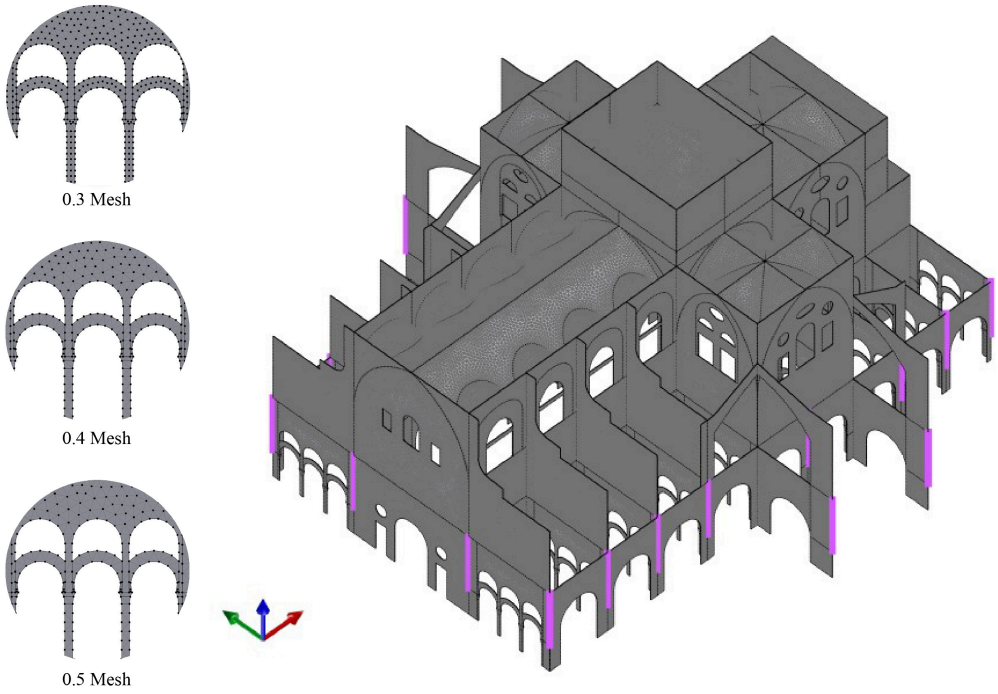


Figure 6. Different FE mesh configurations considered for the sensitivity analysis.

3.2. FE Numerical Model

The geometrical model was imported into STKO [38], where the FE discretization has been generated and subsequently analyzed using the OpenSees computational framework.

A macro-modelling strategy was adopted, in which the different masonry typologies were represented as homogeneous. This approach was selected because the objective of the model is to investigate the global dynamic behavior of a large and geometrically complex monument rather than the response of individual masonry units and mortar joints. Owing to the highly irregular geometry, the structure was discretized using the three-node triangular shell element ShellDKGT, available in OpenSees. Each structural component was assigned a PlateFiberSection with the corresponding thickness and constitutive material reported in Figure 5b and Table 1.

Table 1. Mechanical properties adopted for the different materials considered in the FE model. ρ, density; E, Young's modulus; v, Poisson ratio; f_t, tensile strength; G_t, tensile fracture energy; f_{cp}, peak compressive strength; ε_{cp}, compressive strain at peak strength; G_c, compressive fracture energy.

Material	Application	ρ [kg/m^3]	E [GPa]	v	f_t [MPa]	G_t [kPa]	f_{cp} [MPa]	ε_{cp}	G_c [kPa]
Marble/ Granite	Mosque's arcade columns	2800	29	0.25	3	0.529	60	0.02	800
Limestone masonry	Mosque walls	1800	1.80	0.30	0.10	0.304	2.78	0.0042	235
	Cathedral walls, pilasters and buttresses	1600	1.30	0.30	0.26	0.300	2.60	0.0042	30.06
Brick masonry	Arcades (Mosque) Dome's cover and central nave buttresses (Cathedral)	1800	1.50	0.20	0.21	0.318	3.57	0.0024	31.82
			1.80	0.20	0.43	0.329	4.30	0.0024	32.91

A mesh sensitivity analysis has been carried out to evaluate the influence of the element size on the predicted dynamic response. Six characteristic mesh sizes (0.25, 0.30, 0.35, 0.40, 0.45 and 0.50 m) have been considered, and the final discretization (0.3 m) has been selected as a compromise between numerical accuracy and computational cost. The resulting FE mesh as well as some details to the mesh configurations selected are shown in Figure 6.

3.3. Material Constitutive Models

The nonlinear behavior of the mechanical materials was represented using the damage-plasticity 'ASDEADamageTC3' constitutive model available in OpenSees [39]. The material combines isotropic damage under tension and compression, enabling the progressive degradation of stiffness associated with cracking and crushing phenomena while preserving computational efficiency for large-scale nonlinear analyses. The 'PlateFiberSection' element has been used to construct a membrane-plate fiber section for the shell elements.

The mechanical properties adopted in the present model were based on previous experimental characterization performed by the authors in the Mosque–Cathedral of Córdoba [23]. The experimental campaign included rebound hammer tests on the columns and on the main limestone and brick masonry typologies to estimate their compressive strength. Ambient-vibration tests were subsequently conducted on the arcades to characterize their dynamic behavior and provide information for the definition of the dynamic material properties and contact-interface parameters. Although the experimental campaign was conducted in another sector of the monument, the investigated materials and construction typologies are also present in the Gothic–Renaissance crossing and therefore provide building-specific reference values for the present FE model. For properties not directly obtained experimentally, such as tensile strength and strain at peak compressive strength,

values were derived from established literature relationships and the Italian Building Code [40], as described below.

Distinct constitutive material definitions were assigned to the principal masonry and stone typologies identified in the monument. Marble and granite were assigned to the preserved Islamic columns; limestone masonry to the walls, piers and buttresses; and brick masonry to the brick arches, vaults, dome covering layer and eight buttresses connected to the main nave.

The mechanical properties assigned to the different structural materials have been established according to the available level of knowledge for each construction phase and are summarized in Table 1. For the original Islamic structure, including the marble and granite columns, limestone masonry, and brick masonry, the material parameters have been adopted from previous experimental and numerical investigations carried out by the authors on the building [23].

For the Gothic–Renaissance crossing, where direct experimental characterization is not available, the initial mechanical properties have been selected from the reference values provided by the Italian Building Code (NTC 2018) [40] (density, ρ, Young Modulus, E, and compressive strength, f_{cp}). The masonry typologies adopted have been chosen to best represent the constructive characteristics of the monument, namely *muratura in mattoni pieni e malta di calce* for the brick masonry and the closest equivalent category for the limestone masonry.

Because direct experimental characterization of all constitutive parameters was not available, several material properties have been estimated following well-established assumptions reported in the literature. The tensile strength f_t has been assumed as a 10% of f_{cp}, consistently with previous applications to masonry structures [41]. Likewise, the strain corresponding to the peak compressive strength (ε_{cp}), has been selected within the experimentally based ranges reported in previous studies [42].

The tensile and compressive fracture energies, G_t and G_c, were selected following Petracca et al. [43] formulation. The initial, f_{c0}, and the residual, f_{cr}, compressive strengths were defined as 50% and 10% of the adopted f_{cp}, respectively.

These assumptions allow the nonlinear behavior of masonry to be represented while acknowledging the unavoidable uncertainties associated with the mechanical characterization of heritage materials.

The adopted material properties constitute the reference mechanical characterization of the FE model. Their influence on the predicted dynamic response is subsequently evaluated through the sensitivity analyses presented in Section 4.2.1.

3.4. Boundary Conditions

The structural interaction between the Gothic–Renaissance crossing and the pre-existing Islamic structure has been explicitly represented through interface elements to account for the mechanical behavior of the connections between masonry components belonging to different construction phases.

To simulate these interfaces, the 'ZeroLengthContactASDimplex' element available in OpenSees has been adopted. The element has been introduced at the interfaces in both X and Y (when applicable) between the Gothic–Renaissance crossing and the surrounding Islamic structure, respecting the existing geometry and current structural configuration (Figure 6).

The constitutive behavior of the contact interfaces is governed by the friction coefficient (μ), cohesion (c), and the normal and tangential penalty stiffnesses (K_n and K_t, respectively). The values have been selected according to recommendations available in the literature for historical masonry [24]. A friction coefficient of μ = 0.50 has been adopted,

corresponding to masonry with regular bonding and relatively good mortar quality. The cohesion has been assumed as 0.10 MPa, which lies within the range commonly reported for historic masonry.

K_n and K_t control the transfer of compressive and shear forces across the interfaces and therefore directly influence the global stiffness of the numerical model. Since these parameters cannot be determined experimentally, they have been considered from reference experimental testing on masonry units [44]. These values equal to $K_n = 2.0 \times 10^9$ kPa/m and $K_t = 6.0 \times 10^8$ kPa/m, respectively, also based on a previous study by the authors [45], concerning stone-column assemblies in the Mosque–Cathedral of Córdoba and implemented within the same OpenSees and STKO framework.

The base of the model has been assumed to be fully restrained. The model adopts fully restrained boundary conditions at foundation level as a modelling assumption. Soil–structure interaction was outside the scope of the present work. Consequently, the reported modal properties should be interpreted as fixed-base estimates. Its influence will be assessed in future work through an extended soil–foundation–structure model.

4. Numerical Results and Dynamic Characterization

All numerical analyses have been carried out in OpenSees framework through the STKO interface. The simulations have been performed on a workstation equipped with a 13th Intel® Core™ i7-13700 processor operating at 2.10 GHz and 16 GB of RAM. Eigenvalue analyses have been conducted using the genBandArpack eigensolver. The parallel Reverse Cuthill–McKee (RCM) algorithm has been adopted to renumber the degrees of freedom and minimize the bandwidth of the global stiffness matrix. The MUMPS sparse direct solver has been employed for solving the resulting linear system. Boundary constraints have been enforced using the Penalty Method with penalty factors of $\alpha_S = 1 \times 10^{12}$ and $\alpha_M = 1 \times 10^{12}$.

4.1. Global Dynamic Behavior

Following the sensitivity analyses, a modal analysis has been performed to investigate the global dynamic behavior of the Gothic–Renaissance crossing. The three vibration modes, together with their corresponding natural frequencies and modal participation factors, are presented in Table 2. These modes represent the principal translational and rotational mechanisms governing the dynamic response of the structure. Furthermore, they provide insight into the interaction between the Gothic–Renaissance crossing and the surrounding Islamic structural system.

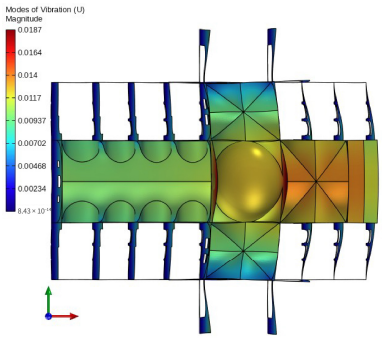
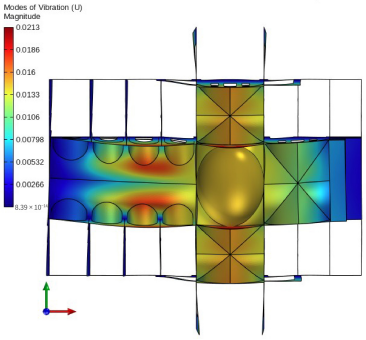
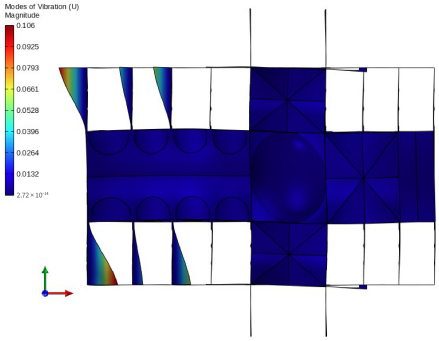
The modes discussed below were selected from the calculated modal range because they represent the dominant global responses of the crossing. Other extracted modes predominantly correspond to localized deformation mechanisms involving individual structural components and exhibit limited modal mass participation.

The results indicate that the dynamic response is dominated by two translational modes. The first mode corresponds to a longitudinal translation (X direction) with a natural frequency of 2.01 Hz and an effective modal mass participation ratio of 62.60%, demonstrating that this direction governs the global response of the crossing. The second mode, associated with transverse translation (Y direction), occurs at 2.52 Hz with a participation factor of 44.06%. The third mode corresponds to a torsional response about the vertical axis Z at 3.14 Hz, exhibiting a rotational participation factor of only 1.02%.

The first vibration mode is characterized by a global longitudinal displacement involving the central dome, the longitudinal nave, the surrounding masonry walls, and the lower Islamic arcades. Rather than exhibiting localized deformations, the displacement field extends continuously throughout the structure, indicating that the crossing behaves

as an integrated structural system. This behavior confirms that the interaction between the Gothic–Renaissance intervention and the pre-existing Islamic structure is sufficiently effective to produce a coupled global response, rather than allowing the two construction phases to vibrate independently. The relatively high modal participation factor (62.6%) further indicates that longitudinal excitation is expected to activate a significant proportion of the structural mass.

Table 2. Global vibration modes and modal participation factors of the FE model.

Mode 1 **Translational X**	**Mode 2** **Translational Y**	**Mode 3** **Rotational**
		
f_1 = 2.01 Hz M_{1x} = 62.6%	f_2 = 2.52 Hz M_{2y} = 44.06%	f_3 = 3.14 Hz RM_{3z} = 1.02%

The second vibration mode corresponds to transverse translation. Although the overall deformation pattern remains global, larger displacements develop in the lateral walls and buttresses, reflecting their greater contribution to the transverse flexibility of the crossing. Compared with the first mode, the natural frequency increases by approximately 25% (from 2.01 Hz to 2.52 Hz), suggesting a stiffer structural response in the transverse direction. Nevertheless, the participation factor decreases to 44.06%, indicating that the associated mass participation is more distributed among higher modes than in the longitudinal direction. This behavior highlights the structural role of the buttresses in controlling transverse deformations generated by the vaulted system and the central dome.

The third mode is associated with torsional motion about the vertical axis. Unlike the previous translational modes, opposite lateral displacements develop on either side of the crossing, producing a coupled rotational mechanism. Despite the approximately symmetric geometry of the crossing, the appearance of torsional behavior indicates that local differences in stiffness and structural connectivity influence the global response. However, the rotational participation factor remains limited (1.02%), indicating that torsional effects are secondary compared with the dominant translational mechanisms.

Overall, the first three global vibration modes demonstrate that the dynamic behavior of the crossing is governed by the interaction between the central dome, the ribbed vaults, the massive masonry walls, and the adjacent Islamic structural system. The deformation patterns extend over the entire structural assembly, confirming that the Gothic–Renaissance crossing cannot be considered an isolated structural component. Instead, its dynamic response is strongly conditioned by its mechanical interaction with the surrounding mosque.

4.2. Sensitivity Analysis

4.2.1. Mesh Sensitivity

A mesh sensitivity analysis has been performed to identify the coarsest discretization capable of accurately reproducing the global dynamic response while maintaining

a reasonable computational cost. Seven mesh sizes, ranging from 0.20 m to 0.50 m, have been initially considered (Figure 6). However, the 0.20 m mesh could not be analyzed due to its excessive computational requirements. Therefore, the comparison presented in Table 3 includes the meshes ranging from 0.25 m to 0.50 m. The first mode corresponds to a longitudinal translation (X direction). The second mode corresponds to the transverse translation (Y direction), and the third mode corresponds to a torsional response about the vertical axis Z, as presented in Section 4.2.

Table 3. Mesh sensitivity analysis of the FE model. Note: The 0.30 m mesh, selected for the subsequent analyses, has been adopted as the reference mesh. The values reported in the Δ_{time} (%) and Δ_f (%) columns are calculated relative to the results obtained for this mesh size.

Mesh Size [m]	N° of Nodes	N° of Element	Total Mass [Tn]	Time [s]	Δ_{time} [%]	Mode 1			Mode 2			Mode 3		
						f_1 [Hz]	M_{1x} [%]	Δ_{f1} [%]	f_2 [Hz]	M_{2y} [%]	Δ_{f2} [%]	f_3 [Hz]	RM_{3z} [%]	Δ_{f3} [%]
0.25	166,750	353,372	18,132.6	5258	+2404%	2.010	62.61	−0.15	2.52	44.06	−0.11	3.14	0.99	−0.15
0.30	120,746	258,587	18,135.1	210	0.00%	2.013	62.6	0.00	2.523	44.06	0.00	3.145	1.02	0.00
0.35	89,330	193,350	18,138.6	146	−30.48%	2.017	62.59	+0.19	2.527	44.06	0.15	3.147	1.04	+0.06
0.40	66,894	146,233	18,141.6	107	−49.05%	2.020	62.58	+0.34	2.531	44.06	0.31	3.149	1.06	+0.12
0.45	55,607	122,407	18,144.5	88	−58.10%	2.023	62.58	+0.49	2.536	44.09	0.51	3.151	1.10	+0.19
0.50	46,354	102,913	18,151.1	74	−64.76%	2.027	62.57	+0.69	2.539	44.08	0.63	3.153	1.10	+0.25

To ensure a consistent comparison, the computational times were obtained from repeated analyses performed under identical hardware and numerical conditions. All calculations used the same OpenSees version, eigensolver, solver, number of processes and number of eigenvalues.

The results showed that mesh refinement has a negligible influence on the predicted modal frequencies. Across the analyzed meshes, the variation in the first three natural frequencies remained below 0.7%, indicating that the global dynamic response had essentially converged even for relatively coarse discretizations. In contrast, the computational effort was highly dependent on the element size. Reducing the mesh size from 0.30 m to 0.25 m increased the computational time from 210 s to 5258 s, corresponding to an increase of approximately 2400%, while improving the predicted frequencies by less than 0.2%. Conversely, increasing the mesh size to 0.50 m reduced the computational time by approximately 65%, although the frequency deviations increased to about 0.6% and the geometric representation became noticeably coarser. The total structural mass also remained practically constant throughout the analyzed meshes, varying by less than 0.1%. This indicates that the mesh refinement does not significantly modify the inertial properties of the numerical model.

These results indicated that the dynamic response of the model is relatively insensitive to the adopted mesh density once a characteristic element size of approximately 0.30 m is reached. Consequently, the mesh comprising 258,587 shell elements and 120,746 nodes has been adopted for the subsequent analyses, as it provides the best compromise between numerical accuracy, computational efficiency and geometric representation of the complex vaulted geometry.

4.2.2. Sensitivity of the Dynamic Properties

In Figure 7, the influence of the principal mechanical parameters on the predicted dynamic response has been investigated by independently varying the ρ and E by ±5% and ±10%, relative to the baseline values previously reported in Table 1, while keeping all remaining properties unchanged. The ±5% and ±10% variations were selected to evaluate the local sensitivity of the modal response around the adopted reference values.

The baseline properties were primarily derived from previous experimental investigations conducted by the authors on the Mosque–Cathedral and checked against the representative parameters and ranges reported for historical masonry typologies [42].

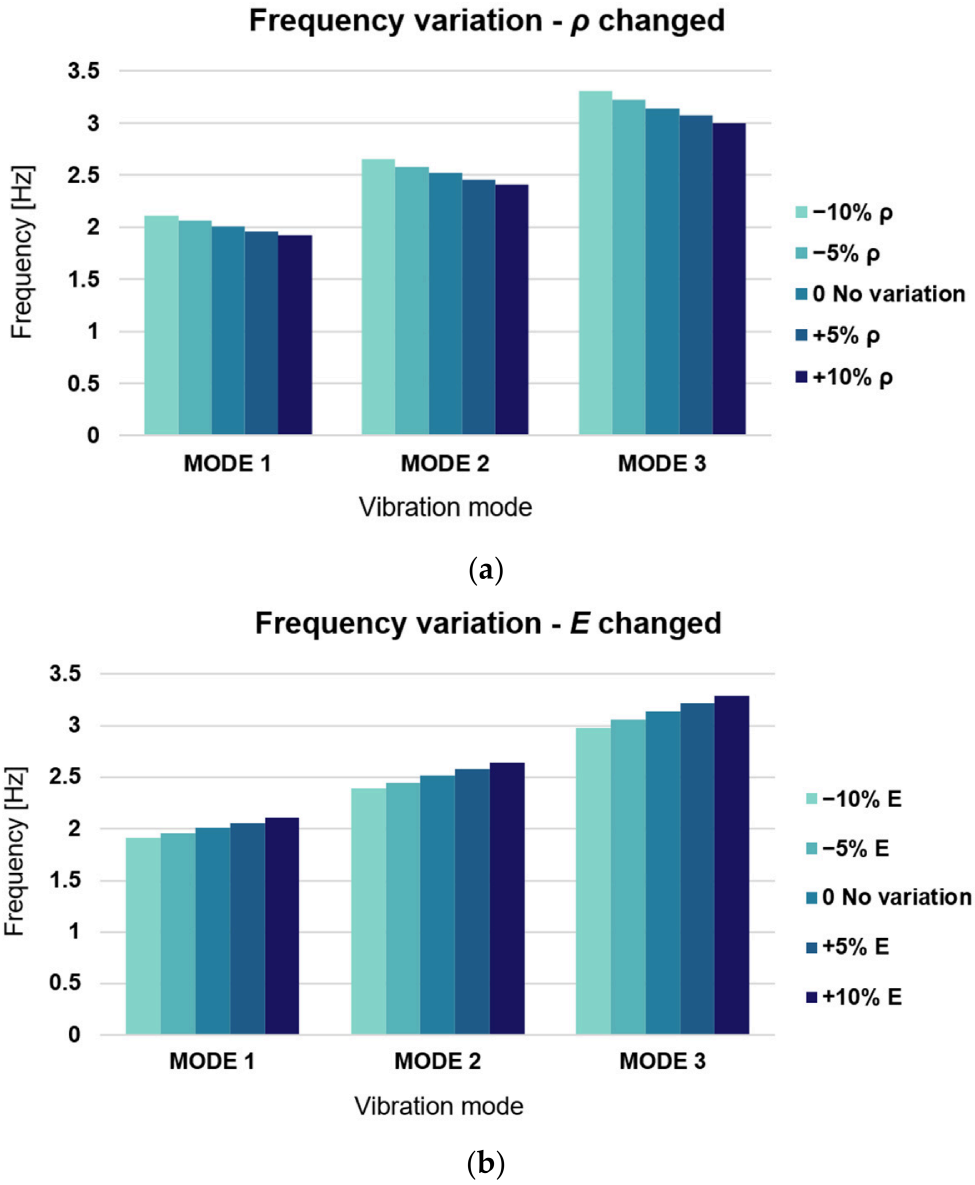


Figure 7. Frequency variation in each vibration mode identified by changing the dynamic properties: (**a**) density, ρ, and (**b**) Young Modulus, E.

The quantitative review of all extracted modes showed that the modes governing the global response retained their translational or rotational classification and similar mass participation ratios for the investigated material-property variations.

As expected, decreasing the material density increased the natural frequencies, whereas increasing the density produced the opposite effect. A 10% reduction in density increased the frequencies of the first three modes by 4.98%, 5.16% and 5.41%, respectively. A 10% increase reduced them by approximately 4.4%. Similarly, modifying the Young's modulus produced an almost symmetrical response. A 10% reduction in E decreased the modal frequencies by approximately 5%, whereas a 10% increase resulted in frequency increments ranging between 4.76% and 4.98%. For both parameters, variations of $\pm$5% produced frequency changes limited to approximately 2.2–2.8%.

An important observation is that the three global vibration modes exhibit almost identical sensitivity to both parameters. The maximum difference between the frequency variations in the three modes remains below 0.5%, indicating that moderate uncertainties in density or elastic stiffness mainly modify the global stiffness-to-mass ratio without altering the modal hierarchy. Therefore, the adopted material properties primarily affect the absolute frequency values rather than the deformation patterns, supporting the robustness of the qualitative interpretation of the global vibration modes presented in the following sections.

4.2.3. Sensitivity of Boundary Conditions

The influence of boundary conditions was evaluated by comparing the current model with different configurations. The same geometry, mesh and material properties were maintained in all cases, modifying only the lateral boundary conditions. The reference model incorporating ZeroLengthContactASDimplex interface elements was compared with a free model restrained only at ground level and a fixed model in which the interface boundaries were fully restrained.

Table 4 compares the frequencies and modal mass participation ratios of the representative translational and rotational modes.

Table 4. Comparison of the representative X-translational, Y-translational and rotational modes for the free, contact and fixed boundary-condition configurations.

Configuration of the Boundary Conditions	Mode 1 Translational X	Mode 2 Translational Y	Mode 3 Rotational
Free	f_1 = 1.22 Hz M_{1x} = 67.6%	f_2 = 1.77 Hz M_{2y} = 71.26%	f_3 = 2.05 Hz RM_{3z} = 52.14%
Contact	f_1 = 2.01 Hz M_{1x} = 62.6%	f_2 = 2.52 Hz M_{2y} = 44.06%	f_3 = 3.14 Hz RM_{3z} = 1.02%
Fixed	f_1 = 2.02 Hz M_{1x} = 61.96%	f_2 = 2.53 Hz M_{2y} = 43.96%	f_3 = 3.19 Hz RM_{3z} = 0.47%

Removing the lateral interaction produces a substantial reduction in the modal frequencies. Relative to the contact model, the frequencies of the free configuration decrease by approximately 39.1%, 29.6% and 34.6% for the X-translational, Y-translational and comparable rotational modes, respectively. The free model also exhibits a different distribution of modal mass, particularly in the rotational response, whose participation increases to 52.14%. These results indicate that disregarding the connection with the surrounding Islamic structure significantly modifies both the stiffness and the global response of the crossing.

Conversely, the contact and fixed configurations present similar translational mode shapes and frequencies. Relative to the contact model, fully restraining the interfaces increases the three selected frequencies by only approximately 0.6%, 0.3% and 1.7%, respectively. The translational modal mass ratios are also similar in both models. This indicates that the contact formulation provides sufficient lateral restraint to reproduce a global translational response close to that of the fixed-interface configuration. Nevertheless, differences remain in the rotational response and in some local displacement patterns, showing that the contact and fixed assumptions are not mechanically equivalent.

4.3. Influence of the Buttress Configuration

Buttresses play a fundamental role in the structural equilibrium by providing lateral restraint and transferring horizontal thrusts towards the supporting piers, walls, and foundations. Their structural effectiveness depends on their geometry, stiffness, connection with the adjacent walls and arches, and modifications introduced during the historical evolution of the building. Recent research on the Süleymaniye Mosque, located in Istanbul, demonstrated the importance of the buttress system by comparing the existing configuration with hypothetical models incorporating reduced or eliminated buttress depths [46].

As shown in Figure 8, the four buttresses connected to the main nave were originally open but were later infilled with masonry arches as part of a later strengthening intervention. The four buttresses of the opposite side were also enclosed. These differences provide the basis for comparing the existing configuration with a hypothetical model in which the central buttresses are also fully infilled.

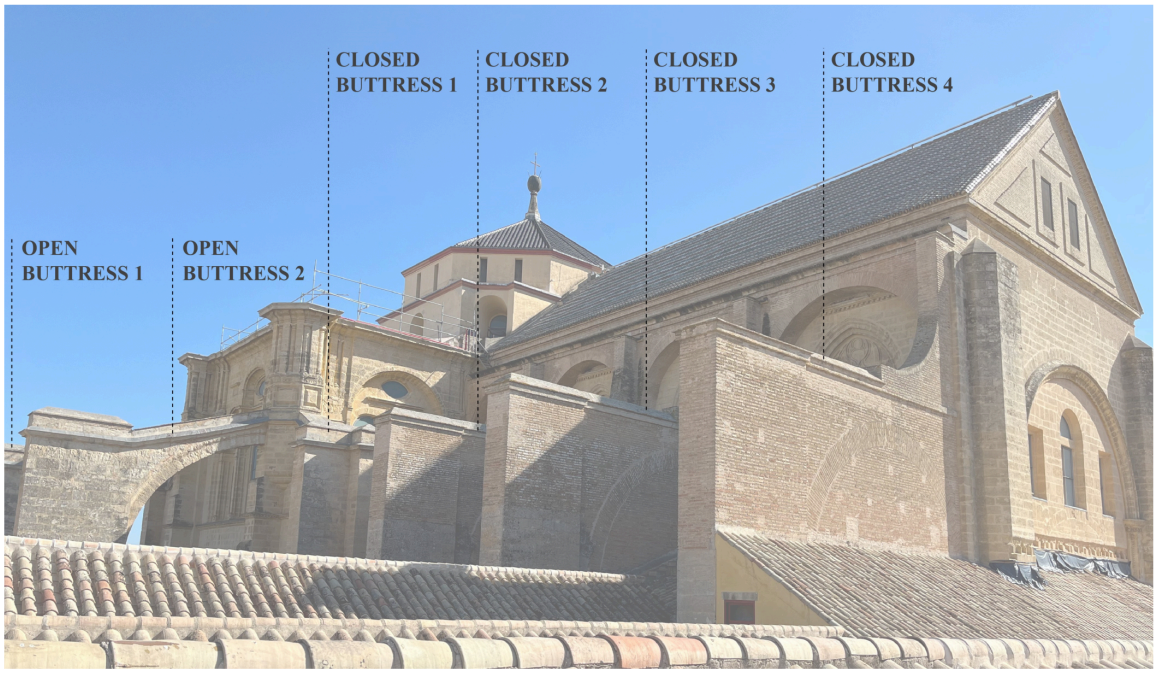


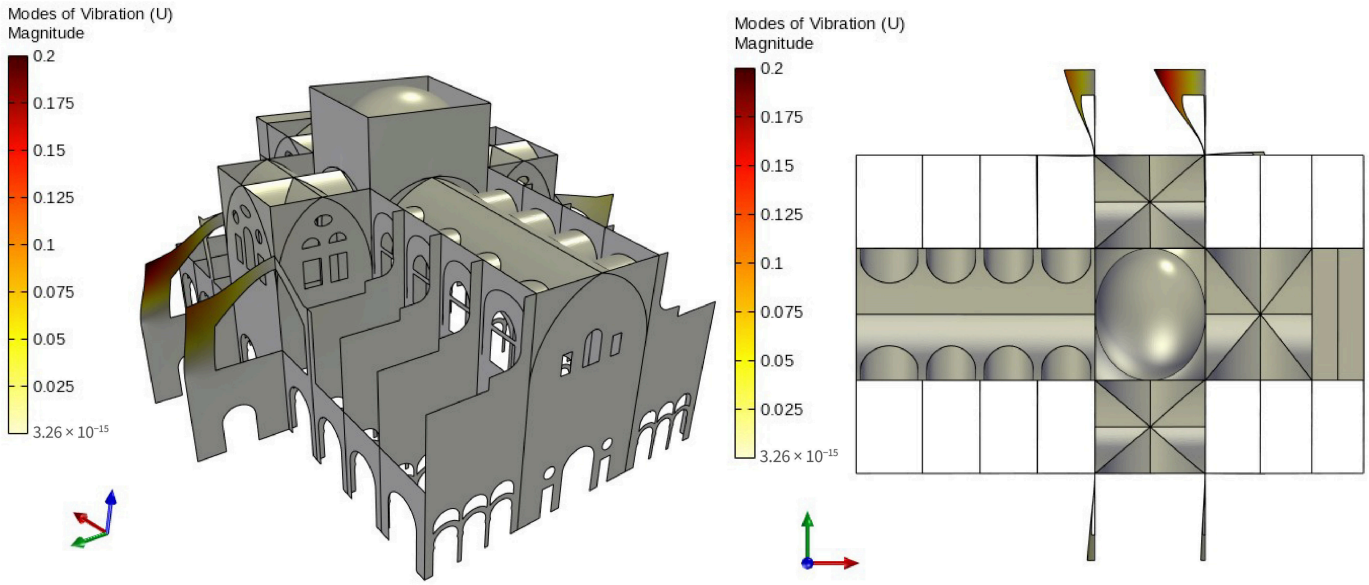
Figure 8. Buttresses of the Gothic–Renaissance crossing showing the infilled and open openings. Picture taken by the authors.

4.3.1. Existing Configuration

In addition to the principal global vibration modes, the modal analysis also identifies local deformation mechanisms involving these individual structural components of the Gothic–Renaissance crossing. Although these local modes contribute only marginally to the overall dynamic response, they provide valuable information regarding the spatial distribution of stiffness and the structural interaction between the different construction phases. Figure 9 illustrates one of the local vibration mechanisms identified in the numerical analysis, selected due to the concentration of localized deformation in the buttresses of the central part of the monument.

The modal results are consistent with the historical evolution of the monument. These modifications likely increased the local stiffness of the affected buttresses, thereby reducing their participation in the identified local vibration mechanisms. In contrast, the two buttresses that remain open on the side shown in Figure 8, together with their corresponding counterparts on the opposite side, retain greater structural flexibility and consequently experience larger local displacements during vibration. The open configuration, geometrical

discontinuities and reduced lateral restraint of the central buttresses identify them, from a qualitative structural assessment, as potentially critical areas. Therefore, the predicted deformation patterns reflect not only the current structural configuration of the crossing, but also the mechanical consequences of the successive historical interventions that have modified its stiffness distribution.



(**a**) (**b**)

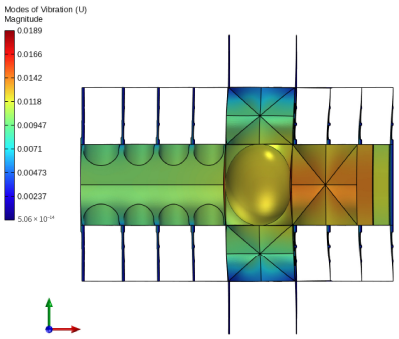
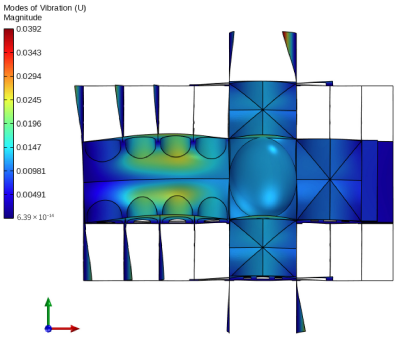
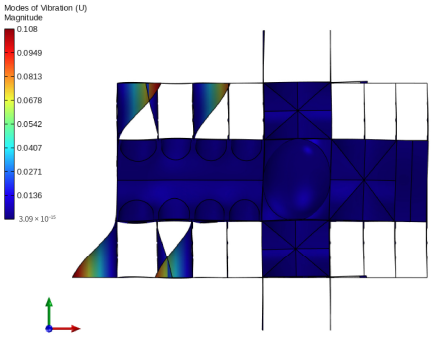
Figure 9. Local vibration mechanism identified in the modal analysis. f_L = 2.31 Hz. (**a**) three-dimensional view of the modal deformation concentrated in the buttresses, and (**b**) plan view of the same vibration mode.

4.3.2. Hypothetical Infilled Configuration

To assess the influence of the buttress configuration, an additional model was analyzed in which the central buttresses were hypothetically considered fully infilled, while maintaining the same mesh, material properties and boundary conditions (Table 5). The principal modes retained their global translational and rotational character. However, their frequencies increased from 2.01, 2.52 and 3.14 Hz in the current configuration to 2.03, 2.96 and 3.17 Hz, respectively, indicating an increase in global stiffness. The modal mass participation ratios changed from 62.60% to 60.66% for the X-translational mode and from 44.06% to 37.99% for the Y-translational mode, whereas the rotational participation of the third mode increased from 1.02% to 2.22%. These results indicate that infilling the central buttresses increases lateral restraint and modifies the modal response, particularly in the Y direction, which exhibited reduced deformation within the crossing.

From a structural perspective, these results indicate that the local dynamic response is strongly influenced by stiffness discontinuities associated with the successive construction phases. Whereas the first vibration modes demonstrate that the Gothic–Renaissance crossing and the surrounding Islamic structure behave as an integrated structural system, the higher modes reveal that individual structural components remain sensitive to local variations in stiffness and connectivity. This observation highlights the importance of explicitly representing the interfaces between successive construction phases when modelling historically layered monuments.

Table 5. Global vibration modes and modal participation factors of the Gothic–Renaissance crossing FE model, with hypothetical infilled buttresses configuration.

Mode 1 **Translational X**	**Mode 2** **Translational Y**	**Mode 3** **Rotational**
		
f_1 = 2.03 Hz M_{1x} = 60.66%	f_2 = 2.96 Hz M_{2y} = 37.99%	f_3 = 3.17 Hz RM_{3z} = 2.22%

The identified local vibration mechanisms also provide useful information for future structural assessment and monitoring. Although they have a limited influence on the global response, they identify structural components that may be more susceptible to local deformation accumulation under long-term environmental actions or seismic loading. Consequently, the buttresses exhibiting the largest modal displacements represent suitable locations for future monitoring systems and targeted structural inspections.

These findings are consistent with observations reported for the continuous dynamic monitoring of the Milan Cathedral [47]. In that study, eight global vibration modes were identified within the 1–5 Hz frequency range, with the first two modes corresponding predominantly to transverse and longitudinal sway. Although a direct comparison is not appropriate because of the different dimensions, structural configurations and portions of the monuments analyzed, both studies reveal well-defined vibration mechanisms associated with the principal structural directions. As reported for the Milan Cathedral, the identification and interpretation of higher modes are inherently more challenging because of their greater spatial complexity and sensitivity to the sensor arrangement. Furthermore, the ambient frequency variations observed in that study indicate that moderate discrepancies between numerical predictions and future experimental measurements should not necessarily be attributed solely to modelling assumptions.

5. Conclusions

5.1. Key Points

This study presents the first 3D FE model of the Gothic–Renaissance crossing of the Mosque–Cathedral of Córdoba, explicitly representing the mechanical interaction between the Christian intervention and the surrounding Islamic structure through frictional contact interfaces. The proposed modeling strategy addresses one of the principal challenges in the numerical assessment of historically superimposed monuments, namely the realistic representation of the structural interaction between successive construction phases.

The sensitivity analyses quantified the influence of the principal modelling parameters on the predicted dynamic response. A characteristic mesh size of 0.30 m provided the best compromise between computational efficiency and numerical accuracy, preserving both the predicted natural frequencies (variations below 0.7%) and the total structural mass (variation below 0.1%), while substantially reducing the computational cost. Likewise,

variations of ±10% in density and Young's modulus modified the predicted frequencies by only approximately 5%, while preserving modal shapes.

Regarding the boundary condition analysis, the results demonstrate that the representation of the lateral interaction is relevant, while the reference contact model provides an intermediate and mechanically more realistic condition between completely free and fully fixed interfaces.

The modal analysis revealed that the first three global vibration modes correspond to two dominant translational modes (2.01 Hz and 2.52 Hz) followed by a torsional mode (3.14 Hz). The modes with the largest modal mass participation involve simultaneous global deformation of the Gothic–Renaissance crossing and the surrounding Islamic structure, while modes dominated by individual components exhibit a local character and lower modal mass participation. The associated modal shapes demonstrate that the Gothic–Renaissance crossing and the surrounding Islamic structure behave as a single integrated structural system rather than as independent construction phases. Consequently, the mechanical interaction between the historical additions plays a fundamental role in the global dynamic behavior and should be explicitly represented in finite element models of similar monuments.

Beyond the global response, the higher vibration modes revealed localized deformation mechanisms concentrated in the buttresses. These local mechanisms were found to be consistent with the historical evolution of the monument, since the buttresses that were subsequently infilled exhibit greater stiffness and reduced modal participation than those that remain open. As a result, the identified local vibration mechanisms provide valuable information for future structural assessment by highlighting structural components that may be more susceptible to the activation of local deformation mechanisms and localized dynamic-response patterns.

5.2. Future Works

This work provides the basis for a detailed three-dimensional FE model of the Gothic–Renaissance crossing, which had not previously been developed, together with a preliminary characterization of its modal response and the sensitivity of its dynamic properties to the main modeling parameters.

Although previous investigations of the monument provided building-specific information on its materials, experimental modal data for the crossing are not currently available. Future research will therefore include a dedicated validation and model-updating phase, following the general principle of integrating experimental evidence with numerical modelling adopted in previous structural studies [48]. Further ambient-vibration testing and Operational Modal Analysis will be used to compare the measured and predicted frequencies and mode shapes and to update the principal mechanical and interface parameters.

The validation process will also consider the uncertainties associated with environmental variability, geometrical idealization and sensor configuration. Repeated measurements under different conditions will help distinguish ambient frequency variations from discrepancies associated with modelling assumptions. After validation, nonlinear static and dynamic analyses will be conducted to investigate structural capacity and potential failure.

Further numerical developments will address modelling assumptions not fully examined in the present study. A dedicated interface sensitivity analysis will evaluate the influence of the normal and tangential penalty stiffnesses, K_n and K_t, on the modal response.

Soil–structure interaction will also be investigated by comparing the current fixed-base model with an extended model incorporating the foundations and surrounding soil.

Finally, the proposed workflow could be applied to other heritage structures to assess its broader transferability. In historically layered monuments, the interface-modelling stage can be adapted to their construction sequence and connection conditions, whereas in single-phase buildings it may be omitted while retaining the geometrical reconstruction, material characterization, sensitivity analysis and validation stages.

Author Contributions: Conceptualization, N.F.-P., M.V.R.-G.-C. and A.M.-E.; methodology, N.F.-P., I.G.-d.-L. and M.V.R.-G.-C.; software, N.F.-P., I.G.-d.-L. and M.V.R.-G.-C.; validation, N.F.-P.; formal analysis, N.F.-P.; investigation, N.F.-P.; resources, N.F.-P., I.G.-d.-L. and M.V.R.-G.-C.; data curation, N.F.-P.; writing—original draft preparation, N.F.-P. and M.V.R.-G.-C.; writing—review and editing, N.F.-P., M.V.R.-G.-C., I.G.-d.-L. and A.M.-E.; visualization, N.F.-P.; supervision, M.V.R.-G.-C. and A.M.-E.; project administration A.M.-E.; funding acquisition, A.M.-E. All authors have read and agreed to the published version of the manuscript.

Funding: This manuscript is part of the R + D + i project "Metodología avanzada para la evaluación de la seguridad estructural y sísmica de edificios patrimoniales". Grant 'Proyecto PID2023-150771OB-I00' funded by MICIU/AEI/10.13039/501100011033 and by FEDER, UE. Natalia Fernández-Pérez (author) wishes to acknowledge the financial support provided by the FPU Programme of Spain's Ministry of Science, Innovation and Universities (FPU24/00143).

Data Availability Statement: The raw data supporting the conclusions of this article will be made available by the authors on request.

Acknowledgments: The authors would like to thank the Cathedral of Córdoba's Chapter for the support and for enabling the study of the monument. Finally, we would like to thank the architect Gabriel Rebollo Puig for his support and help.

Conflicts of Interest: The authors declare no conflicts of interest.

References

1. Puncello, I.; Caprili, S. Seismic Assessment of Historical Masonry Buildings at Different Scale Levels: A Review. *Appl. Sci.* **2023**, *13*, 1941. [CrossRef]
2. Ravichandran, N.; Losanno, D.; Parisi, F. Comparative Assessment of Finite Element Macro-Modelling Approaches for Seismic Analysis of Non-Engineered Masonry Constructions. *Bull. Earthq. Eng.* **2021**, *19*, 5565–5607. [CrossRef]
3. Funari, M.F.; Hajjat, A.E.; Masciotta, M.G.; Oliveira, D.V.; Lourenço, P.B. A Parametric Scan-to-FEM Framework for the Digital Twin Generation of Historic Masonry Structures. *Sustainability* **2021**, *13*, 11088. [CrossRef]
4. Wang, Y.; Gu, Y.; Liu, J. A Domain-Decomposition Generalized Finite Difference Method for Stress Analysis in Three-Dimensional Composite Materials. *Appl. Math. Lett.* **2020**, *104*, 106226. [CrossRef]
5. Kabir, H.; Aghdam, M.M. A Robust Bézier Based Solution for Nonlinear Vibration and Post-Buckling of Random Checkerboard Graphene Nano-Platelets Reinforced Composite Beams. *Compos. Struct.* **2019**, *212*, 184–198. [CrossRef]
6. Leonardi, M.L.; Granja, J.; Oliveira, D.V.; Azenha, M. Scalable BIM Based Open Workflow for Structural Analysis of Masonry Building Aggregates. *Comput. Struct.* **2024**, *297*, 107321. [CrossRef]
7. Saloustros, S.; Pelà, L.; Roca, P. Nonlinear Numerical Modeling of Complex Masonry Heritage Structures Considering History-Related Phenomena in Staged Construction Analysis and Material Uncertainty in Seismic Assessment. *J. Perform. Constr. Facil.* **2020**, *34*, 04020096. [CrossRef]
8. Ghezelbash, A.; Sharma, S.; D'Altri, A.M.; Lourenço, P.B.; Rots, J.G.; Messali, F. Challenges in High-Fidelity Implicit Block-Based Numerical Simulation of Dynamic Out-of-Plane Two-Way Bending in Unreinforced Brick Masonry Walls. *Earthq. Eng. Struct. Dyn.* **2025**, *54*, 1836–1858. [CrossRef]
9. Roca, P.; Cervera, M.; Gariup, G.; Pela', L. Structural Analysis of Masonry Historical Constructions. Classical and Advanced Approaches. *Arch. Comput. Methods Eng.* **2010**, *17*, 299–325. [CrossRef]
10. Meoni, A.; D'Alessandro, A.; Mattiacci, M.; García-Macías, E.; Saviano, F.; Parisi, F.; Lignola, G.P.; Ubertini, F. Structural Performance Assessment of Full-Scale Masonry Wall Systems Using Operational Modal Analysis: Laboratory Testing and Numerical Simulations. *Eng. Struct.* **2024**, *304*, 117663. [CrossRef]
11. Pirchio, D.; Walsh, K.Q.; Kerr, E.; Giongo, I.; Giaretton, M.; Weldon, B.D.; Ciocci, L.; Sorrentino, L. Integrated Framework to Structurally Model Unreinforced Masonry Italian Medieval Churches from Photogrammetry to Finite Element Model Analysis through Heritage Building Information Modeling. *Eng. Struct.* **2021**, *241*, 112439. [CrossRef]

12. Ferrante, A.; Giordano, E.; Clementi, F.; Milani, G.; Formisano, A. FE vs. DE Modeling for the Nonlinear Dynamics of a Historic Church in Central Italy. *Geosciences* **2021**, *11*, 189. [CrossRef]
13. Romero-Sánchez, E.; Morales-Esteban, A.; Bento, R.; Navarro-Casas, J. Numerical Modelling for the Seismic Assessment of Complex Masonry Heritage Buildings: The Case Study of the Giralda Tower. *Bull. Earthq. Eng.* **2023**, *21*, 4669–4701. [CrossRef]
14. Angjeliu, G.; Coronelli, D.; Cardani, G. Model Calibration in Complex Historical Masonry Structures: The Case of Milan Cathedral. In *Proceedings of the 18th World Conference on Earthquake Engineering (WCEE 2024)*; International Association of Earthquake Engineering (IAEE): Tokyo, Japan, 2025; pp. 1–8.
15. Parent, T.; Morenon, P.; Nougayrede, P.; Taforel, P.; Dubois, F.; Morel, S. On the Benefits of the Use of Complementary Numerical Models for the Structural Analysis of a Historic Masonry Monument: Application to a Sexpartite Vault of Notre-Dame de Paris Cathedral. *Int. J. Solids Struct.* **2025**, *310*, 113224. [CrossRef]
16. Parent, T.; Brocato, M.; Colas, A.-S.; Domede, N.; Dubois, F.; Garnier, D.; Gros, A.; Mindeguia, J.-C.; Morel, S.; Morenon, P.; et al. A Multi-Model Structural Analysis of the Vaults of Notre-Dame de Paris Cathedral after the 2019 Fire and a Proposal for a Hybrid Model Merging Continuum and Discrete Approaches. *J. Cult. Herit.* **2024**, *65*, 135–144. [CrossRef]
17. Kesavan, P.; Petracca, M.; Camata, G.; Sethumadhavan, K.; Menon, A. Discontinuum Micromodelling of Unstrengthened and FRCM-Strengthened Masonry Cross-Vaults Subjected to Seismic Excitation. *Int. J. Archit. Herit.* **2024**, *18*, 2004–2022. [CrossRef]
18. Pingaro, N.; Buzzetti, M.; Milani, G. Advanced FE Nonlinear Numerical Modeling to Predict Historical Masonry Vaults Failure: Assessment of Risk Collapse for a Long Span Cloister Vault Heavily Loaded at the Crown by Means of a General-Purpose Numerical Protocol. *Eng. Fail. Anal.* **2025**, *167*, 109070. [CrossRef]
19. Angjeliu, G.; Coronelli, D.; Cardani, G. Numerical Analysis of Mechanical Damage in Ribbed Masonry Vaults under Differential Settlements. *Int. J. Archit. Herit.* **2022**, *16*, 1742–1759. [CrossRef]
20. Malena, M.; Genoese, A.; Panto', B.; Spina, D.; de Felice, G. Two Steps Procedure for the Finite Elements Seismic Analysis of the Casamari Gothic Church. *Buildings* **2022**, *12*, 1451. [CrossRef]
21. Scimemi, G.F.; Giambanco, G.; Spada, A. The Interphase Model Applied to the Analysis of Masonry Structures. *Comput. Methods Appl. Mech. Eng.* **2014**, *279*, 66–85. [CrossRef]
22. Hua, Q.; Chun, Q.; Yuan, Y.; Milani, G. Failure Analysis of Interacting Masonry Arch-Wall Structural Systems: A Micro-Mechanical FEM Insight. *Eng. Fail. Anal.* **2025**, *182*, 110152. [CrossRef]
23. Requena-Garcia-Cruz, M.V.; Romero-Sánchez, E.; Morales-Esteban, A. Contribution of the Soil-Structure Interaction to the Seismic Behaviour of the Mosque-Cathedral of Córdoba. *J. Build. Eng.* **2025**, *110*, 113061. [CrossRef]
24. Requena-Garcia-Cruz, M.V.; Romero-Sánchez, E.; López-Piña, M.P.; Morales-Esteban, A. Preliminary Structural and Seismic Performance Assessment of the Mosque-Cathedral of Cordoba: The Abd al-Rahman I Sector. *Eng. Struct.* **2023**, *291*, 116465. [CrossRef]
25. Requena-Garcia-Cruz, M.; Romero-Sanchez, E.; Morales-Esteban, A. Dynamic Performance of the Mosque-Cathedral of Córdoba under Different Earthquake Scenarios: The Abd al-Rahman I Sector. *J. Build. Eng.* **2023**, *79*, 107853. [CrossRef]
26. Ferrante, A.; Dubois, F.; Morenon, P. Comparison of Continuous and Discrete Modeling Strategies for the Structural Assessment of a Masonry Vault Under Dynamic Seismic Loading. *Int. J. Archit. Herit.* **2024**, *18*, 1873–1885. [CrossRef]
27. McKenna, F.; Fenves, G.L.; Scott, M.H. *OpenSees: Open System for Earthquake Engineering Simulation. In Pacific Earthquake Engineering Research Center*; University of California: Berkeley, CA, USA, 2000.
28. Akan, O.D.; Petracca, M.; Camata, G.; Lai, C.G.; Spacone, E.; Tamagnini, C. An Efficient Finite Element Framework for Nonlinear Seismic Soil-Foundation-Structure Interaction in Shallow-Founded Squat Masonry Structures. *Soil Dyn. Earthq. Eng.* **2026**, *209*, 110520. [CrossRef]
29. Fernández-Pérez, N.; Requena-García-Cruz, M.-V.; Morales-Esteban, A. Understanding the Load Transfer and Seismic Behaviour of a Hybrid Heritage Structure: The Mosque-Cathedral of Córdoba. In *Proceedings of the Resilience, Multi-Risk Assessment and Monitoring—ICONREM 2026*; Tanganelli, M., Viti, S., Arrighi, C., Intrieri, E., Eds.; Springer Nature: Berlin/Heidelberg, Germany, 2026.
30. Cabildo Catedral de Cordoba. Management Plan—Mosque-Cathedral of Cordoba [Plan Director-Mezquita-Catedral de Córdoba]. 2025. Available online: https://mezquita-catedraldecordoba.es/site/assets/files/61555/plan_director_mcdc_2025.pdf (accessed on 15 May 2026).
31. Google View of the Mosque-Cathedral of Córdoba on Google Earth Pro, 37°52′43.9″ N 4°46′45.6″ W. Available online: https://earth.google.com/web/search/Mezquita+de+C%C3%B3rdoba/@37.8786147,-4.77928677,116.9432587a,574.24055313d,35y,13.78683468h,57.58019555t,0r/data=CjsaDQoJL20vMDNjYmtfGAIiJgokCVSHYC6XNkZAESo87ORuMUZAGczipZ9v-yFAIeex08A-0SFAQgIIAToDCgEwQgIIAEoNCP_____wEQAA (accessed on 2 May 2026).
32. Hernández Giménez, F. The Cubit in Arabic Historiography of the Great Mosque of Córdoba: Contribution to the Study of the Monument [El Codo En La Historiografía Árabe de La Mezquita Mayor de Córdoba: Contribución al Estudio Del Monumento]. In *Al-Mulk. Yearbook of Arab Studies*; Real Academy of Córdoba: Córdoba, Spain, 1961; Volume 2, pp. 5–52.

33. Almagro Gorbea, A. Transverse Section of the Gothic-Renaissance Crossing of the Mosque-Cathedral of Córdoba 1948, AA-825_05. Available online: https://www.academiacolecciones.com/arquitectura/inventario.php?id=AA-825_05 (accessed on 6 February 2026).
34. Almagro Gorbea, A. Longitudinal Section of the Gothic-Renaissance Crossing of the Mosque-Cathedral of Córdoba 1948, AA-825_04. Available online: https://www.academiacolecciones.com/arquitectura/inventario.php?id=AA-825_04 (accessed on 6 February 2026).
35. Gimena Córdoba, P. *Form, Space, and Structure in the Transition to the Cordoban Renaissance. Tradition and Innovation in the Architecture of Hernán Ruiz "the Elder." [Forma, Espacio y Estructura en la Transición Al Renacimiento Cordobés. Tradición e Innovación en la Arquitectura de Hernán Ruiz "El Viejo"]*; University of Seville: Seville, Spain, 2014.
36. Autodesk Inc. (Ed.) *Autocad 10: Reference Manual*; Autodesk Inc.: San Francisco, CA, USA, 1988.
37. Ruiz Cabrero, G.; Rebollo Puig, G.; Herrero Romero, S. *Master Plan for the Mosque of Córdoba 2021 [Plan Director Mezquita de Córdoba 2021]*; Cabildo Catedral de Córdoba: Córdoba, Spain, 2021.
38. Petracca, M.; Candeloro, F.; Camata, G. STKO User Manual 2017. Available online: https://037b93fe-93d6-40ed-b7fe-89712cf79c6d.usrfiles.com/ugd/037b93_923618f7c6bb4a88875f91c789dcfa98.pdf (accessed on 12 June 2026).
39. Petracca, M.; Pelà, L.; Rossi, R.; Zaghi, S.; Camata, G.; Spacone, E. Micro-Scale Continuous and Discrete Numerical Models for Nonlinear Analysis of Masonry Shear Walls. *Constr. Build. Mater.* **2017**, *149*, 296–314. [CrossRef]
40. Ministerio delle Infrastrutture e dei Trasporti. Norme Tecniche per le Costruzioni. 2018. Available online: https://www.gazzettaufficiale.it/eli/id/2019/02/11/19A00855/sg (accessed on 14 February 2026).
41. Requena-Garcia-Cruz, M.V.; Cattari, S.; Bento, R.; Morales-Esteban, A. Comparative Study of Alternative Equivalent Frame Approaches for the Seismic Assessment of Masonry Buildings in OpenSees. *J. Build. Eng.* **2023**, *66*, 105877. [CrossRef]
42. Kržan, M.; Gostič, S.; Cattari, S.; Bosiljkov, V. Acquiring Reference Parameters of Masonry for the Structural Performance Analysis of Historical Buildings. *Bull. Earthq. Eng.* **2015**, *13*, 203–236. [CrossRef]
43. Petracca, M.; Pelà, L.; Rossi, R.; Oller, S.; Camata, G.; Spacone, E. Multiscale Computational First Order Homogenization of Thick Shells for the Analysis of Out-of-Plane Loaded Masonry Walls. *Comput. Methods Appl. Mech. Eng.* **2017**, *315*, 273–301. [CrossRef]
44. Ferrante, A.; Loverdos, D.; Clementi, F.; Milani, G.; Formisano, A.; Lenci, S.; Sarhosis, V. Discontinuous Approaches for Nonlinear Dynamic Analyses of an Ancient Masonry Tower. *Eng. Struct.* **2021**, *230*, 111626. [CrossRef]
45. Requena-Garcia-Cruz, M.V.; Gómez-Sánchez, J.C.; Gónzalez-de-León, I.; Morales-Esteban, A. Finite Element Modelling Approaches for Assessing Column Stability in Heritage Structures: A Case Study of the Mosque–Cathedral of Córdoba. *Modelling* **2025**, *6*, 130. [CrossRef]
46. İzol, R.; Gürel, M.A.; Mollamahmutoğlu, Ç.; Avcil, F. Evaluation of the Buttress System of a Great Ottoman Mosque Against Gravity Loads and Horizontal Seismic Forces: The Case of the Istanbul Süleymaniye Mosque. *Buildings* **2025**, *15*, 1360. [CrossRef]
47. Gentile, C.; Ruccolo, A.; Canali, F. Continuous Monitoring of the Milan Cathedral: Dynamic Characteristics and Vibration-Based SHM. *J. Civ. Struct. Health Monit.* **2019**, *9*, 671–688. [CrossRef]
48. Liu, M.; Tian, J.; Zhao, J.; Sun, Y.; Liang, J.; Zheng, Y.; Zhang, W.; Wu, X.; Yuan, J.; Fu, H. Seismic Performance of CFRP-Strengthened Steel Fiber Reinforced Concrete Composite Columns: Experimental, Numerical and Theoretical Analyses. *Constr. Build. Mater.* **2025**, *505*, 144692. [CrossRef]

Disclaimer/Publisher's Note: The statements, opinions and data contained in all publications are solely those of the individual author(s) and contributor(s) and not of MDPI and/or the editor(s). MDPI and/or the editor(s) disclaim responsibility for any injury to people or property resulting from any ideas, methods, instructions or products referred to in the content.